Localization and Tracking of Aortic Valve Prosthesis in 2D Fluoroscopic Image Sequences

M. Karar*[a], C. Chalopin[a], D. R. Merk[a,b], S. Jacobs[b], T. Walther[b], O. Burgert[a] and V. Falk[b]

[a] Innovation Center Computer Assisted Surgery (ICCAS),
Semmelweisstrasse 14, 04103 Leipzig, Germany;
[b] Heart Center Leipzig, Struempellstrasse 39, 04289 Leipzig, Germany

ABSTRACT

This paper presents a new method for localization and tracking of the aortic valve prosthesis (AVP) in 2D fluoroscopic image sequences to assist the surgeon to reach the safe zone of implantation during transapical aortic valve implantation. The proposed method includes four main steps: First, the fluoroscopic images are preprocessed using a morphological reconstruction and an adaptive Wiener filter to enhance the AVP edges. Second, a target window, defined by a user on the first image of the sequences which includes the AVP, is tracked in all images using a template matching algorithm. In a third step the corners of the AVP are extracted based on the AVP dimensions and orientation in the target window. Finally, the AVP model is generated in the fluoroscopic image sequences. Although the proposed method is not yet validated intraoperatively, it has been applied to different fluoroscopic image sequences with promising results.

Keywords: Transapical Aortic Valve Implantation, X-ray Fluoroscopy, Aortic Valve Prosthesis Tracking

1. INTRODUCTION

Transapical aortic valve implantation (TA-AVI) is a new minimally invasive technique to treat aortic stenosis [1]. It has been applied in more than 1000 cases in selected medical centers and is a promising alternative to standard surgical operation. Through a left lateral mini thoracotomy and via the apex, a biological aortic stent-fixed valve is guided using a catheter into the aortic root. After reaching the correct position, the stent-fixed valve prosthesis is deployed via an inflatable balloon to its final diameter, thus fixing the prosthesis to the aortic wall. Once deployed the prosthesis cannot be repositioned. If the aortic valve prosthesis (AVP) is placed too high, the coronary arteries may be blocked, resulting in an emergency sternotomy. If the AVP is placed too low, the mitral valve leaflets might be damaged by the stent. The correct placement of the prosthesis is therefore crucial.

Because the aortic root cannot be observed directly by the surgeon during transapical aortic valve replacement, X-ray fluoroscopy is used as an intraopertive imaging modality [2] as shown in Fig.1. However localization of the AVP or identifying the coronary arteries in 2D fluoroscopic images remains a challenging process [3] because the image contrast is generally low. Moving anatomical structures, catheters and guide wires may overlap the prosthesis which moves very fast due to the blood flow. Moreover the presence of contrast agent may hide the upper part of prosthesis. The coronary ostias are also only visible when the contrast agent is injected.

One of the most clinically used and commercially available prosthesis for transapical aortic valve replacement is Edwards-SAPIEN™ valve as shown in Fig. 2 [4]. This paper proposes therefore a method to locate and track this prosthesis through image sequences. However the proposed method can be also used for locating and tracking other types of clinical prosthesis.

In the literature, there are relatively few methods or algorithms for detecting and/or tracking the guide wire or catheter in 2D fluoroscopic images [5]-[8]. Schoonenberg et al. [5] proposed an adaptive filtering of temporally varying x-ray image sequences during endovascular interventions to improve the visual tracking of catheters by radiologists. Using background subtraction technique, Takmura et al. [6] developed an algorithm to help in navigation of catheters during

*mohamed.karar@iccas.de; phone +49 341 9712020; fax +49 341 9712009; www.iccas.de

Medical Imaging 2009: Visualization, Image-Guided Procedures, and Modeling,
edited by Michael I. Miga, Kenneth H. Wong, Proc. of SPIE Vol. 7261, 72611Q
© 2009 SPIE · CCC code: 1605-7422/09/$18 · doi: 10.1117/12.811509

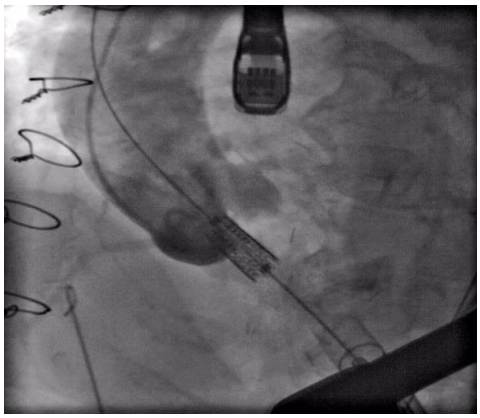

Fig. 1. A 2D fluoroscopic image during transapical aortic valve implantation (TA-AVI).

Fig. 2. Edwards SAPIEN™ valve for TA-AVI.

interventions for intracranial aneurysms on a phantom. However, this algorithm was not totally successful in detecting the microcatheter in all images. Palti-Wasserman et al. [7] suggested an algorithm based on the Hough transform for tracking the guide wire in the coronary arteries to monitor the myocardial function during angioplasty.

One of the effective algorithms for tracking the movement of guide wires or the arteries in X-ray angiography is the template matching [8]-[9]. Baert et al. [8] used the template matching with fitting a spline in the fluoroscopic images for extracting and tracking the guide wire during endovascular interventions. Goszczyńska [9] calculated the coronary blood flow by tracking the coronary arteries movement using the template matching.

To our knowledge, this is the first work concerning the localization and tracking of the AVP in 2D fluoroscopic image sequences for TA-AVI. The main purpose of this paper is therefore to provide an AVP model based assistance to the surgeon, preventing the misplacement of the valve.

2. METHODS

In our developed method, the AVP is located and tracked in 2D fluoroscopic images for TA-AVI. The AVP is assumed to be a rigid object during the localization and tracking process and before inflating the balloon to the prosthesis's final diameter. The algorithm starts with the manual definition by a user of two parameters on the first image of the sequence. First, a region of interest (ROI) of the image which must include the AVP. The ROI is useful to reduce the computing time and increase the algorithm robustness. Second, a quadrangle which fits the AVP edges. The dimensions of the AVP

and its initial orientation are therefore determined after this step. Moreover a target window is also automatically defined. It includes the AVP and is tracked in the sequence in order to overcome the possible rotation of the AVP.

Fig. 3 shows the four main steps of the developed method for localization and tracking the AVP: (1) preprocessing the input fluoroscopic images to filter the image noise and overcome the blurred vision, (2) tracking the prosthesis in the target window using the template matching, (3) extract the corner points of the AVP based on a proposed AVP model, and (4) the AVP model is generated which fits the prosthesis in the fluoroscopic images as a final stage.

2.1 Preprocessing

It's necessary to filter the fluoroscopic images in order to reduce the image noise, to adjust intensities within the image sequence and to enhance the AVP edges with preserving image features. Therefore the input images are preprocessed using a morphological reconstruction operation and an adaptive Wiener filter.

Morphological reconstruction operation removes all the intensity fluctuations except the intensity peak of the mask image (i.e. the fluoroscopic image) by the marker image [10, 11]. The marker image is generated by subtracting a constant value (e.g. 100) from the mask image. Morphological processing starts at the peak in the marker image and spreads throughout the rest of the image based on a 8-connected neighborhood [11]. Then the adaptive Wiener filter is applied to the reconstructed images to overcome the problem of blurred vision [12]. It is more selective than a comparable linear filter and requires therefore more computation time [11].

2.2 Target Window Tracking

The target window of AVP, estimated in the first image, is then tracked within all images of the sequence using the template matching algorithm. It is performed based on the computation of the fast normalized cross correlation (FNCC) [13]. It involves intensities comparison of the target window with the current image of sequence (ROI). Although the intensities of two images could be different, a high similarity will be obtained because they represent the same AVP [14]. The equation for 2D normalized cross-correlation is given by [13]:

$$M(u,v) = \frac{\sum_{x,y}[r(x,y) - \bar{r}_{u,v}][t(x-u, y-v) - \bar{t}]}{\sqrt{\sum_{x,y}[r(x,y) - \bar{r}_{u,v}]^2 \sum_{x,y}[t(x-u, y-v) - \bar{t}]^2}} \quad (1)$$

where r is the ROI and t is the target window. The sum is over the coordinates x and y of ROI. t is positioned at (u,v). $\bar{r}_{u,v}$ and $\bar{t}$ are the mean brightness value of r and t respectively. The normalized cross correlation coefficient M provides

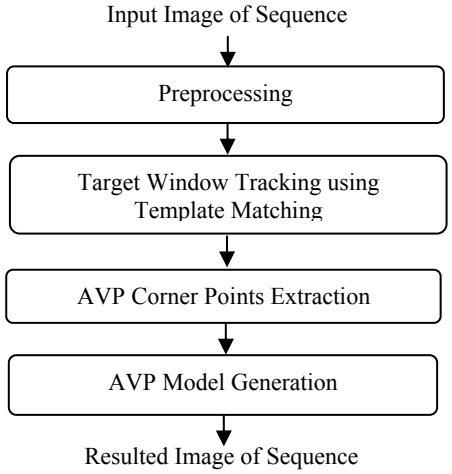

Fig. 3. Main steps of the aortic valve prosthesis (AVP) localization and tracking method.

a similarity coefficient between both images. The result of FNCC returns the maximum value M_{max}. The location at $(u, v)|_{Mmax}$ of the target window in the current image show the best matching location of the new target window [9]. It is assumed to be the center of the target window and also the center of the AVP.

It is clear that the template matching is not enough for extracting the corner points of the AVP. The matching process is not invariant to the fast motion and small orientation changes of the AVP. Moreover the presence of contrast agent may occlude the upper part of the prosthesis. Therefore these limitations have been solved using a proposed AVP model to locate the prosthesis within the target window as presented in the following section.

2.3 AVP Corner Points Extraction

The Canny filter is then applied on the new target window to detect the AVP edges [15]. However, due to the presence of contrast agent or the overlapped catheter, all edges can't be extracted. Therefore we proposed an AVP model which represents the fixed dimensions of the prosthesis estimated in the first image of sequence as shown in Fig. 4 (a).

In Fig. 4 (b), the proposed AVP model is a semi-rectangle with l, the AVP length, and w_1 and w_2, respectively the upper and lower widths. The AVP corner points are noted p_1, p_2, p_3, and p_4. The angle φ indicates the constant angle between the two segments (p_1-p_3) and (p_1-p_4) to keep the shape of the AVP constant through the sequence. The angle Θ between (c-p_1) and the horizontal line represents the orientation of the prosthesis. The AVP corner points are extracted based on the AVP model as follow:

i) Estimation of p_1 position:
Since the AVP resides at the beginning of aortic root, it is always showed that the orientation of the AVP is around 45 degree in 2D fluoroscopic images. Therefore the point in the target window with the maximum x-coordinate value and belonging to the AVP edge represents the corner point p_1.

ii) Estimation of the AVP orientation Θ:
To show the orientation changes of prosthesis through the sequence, the orientation difference $\Delta\Theta_i$ is calculated between two consecutive images as:

$$\Delta\theta_i = \theta_i - \theta_{i-1}, \qquad i = 2 \ldots n \tag{2}$$

where Θ_i and Θ_{i-1} are the AVP orientation in the current image i and in the previous image i-1. n is the number of images in the sequence.

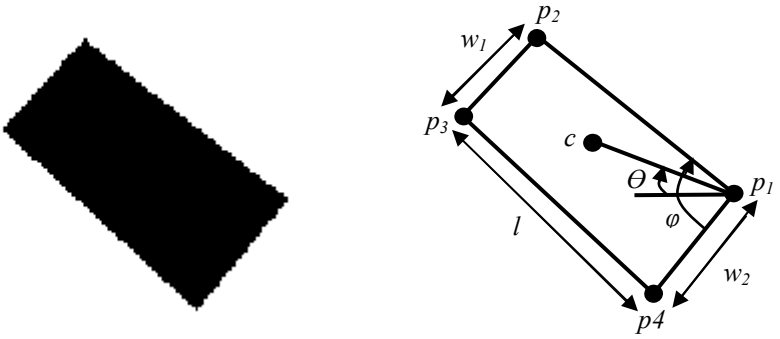

Fig. 4. (a) A binary mask image of the AVP is generated from a quadrangle selected by the user, to define the required parameters of the AVP, (b) The AVP model includes the AVP dimensions and orientation: the length l, the upper and lower widths are $w1$ and $w2$ respectively. p_1, p_2, p_3, and p_4 are the corner points. The angle φ indicates the constant shape angle of the AVP. The angle Θ represents the AVP orientation in the current image of sequence.

iii) Estimation of the positions of p_2, p_3, and p_4:
The other three corner points: p_2, p_3, and p_4, are obtained by rotating the AVP model in the previous image with $\Delta\Theta_i$. Finally, the AVP model is generated and displayed for all images of the sequence.

3. RESULTS AND DISCUSSION

The developed method for locating and tracking the AVP was implemented using MATLAB® (Image Processing Toolbox™) on a PC with Intel® CPU 2.4 GHz. The execution time of algorithm is approximately one second per frame. Results are shown on three different fluoroscopic image sequences. They were acquired using Siemens C-arm angiography system at the Heart Center Leipzig, Germany. The size of each image is 512×512 pixels. Prosthesis position and dimensions are different according to these sequences.

Table 1 summarizes the data and initial parameters used in the algorithm for the three fluoroscopic image sequences as: the number of frames, the size of the ROI and the size of the target window. The ROI size is automatically initialized to 250×250 pixels, but the user may resize it regarding the AVP dimensions (e.g. ROI is 250×200 pixels for the sequence no. 1). The dimensions and angles of the AVP are estimated from the AVP model as shown in Fig. 4(b).

Table. 1. The predefined parameters used in the algorithm for the three fluoroscopic image sequences

Sequence Number	1	2	3
Number of Frames	76	35	29
Size of the interested area (ROI) (pixels)	250×200	250×250	250×250
Size of the target window (pixels)	77×77	95×107	94×96
Dimensions of the AVP (mm)	$w_1 = 14.55$	$w_1 = 16.50$	$w_1 = 19.21$
	$w_2 = 15.91$	$w_2 = 18.61$	$w_2 = 21.20$
	$l = 32.42$	$l = 40.33$	$l = 40.9$
Fixed angle of AVP (φ)	85.50^{o}	85.00^{o}	89.13^{o}
Initial angle of AVP orientation (Θ_1)	18.97^{o}	15.52^{o}	9.70^{o}

In each frame of the three image sequences, the maximum value of matching M_{max} is recorded as shown in Fig. 5,. M_{max} is used as an index to check the correctness of the template matching. The first image of each sequence shows the best value of matching ($M_{max} = 1$) because the target window is predefined in the first image. The lowest value of M_{max} obtained for the three sequences is 0.58 (21st image of sequence no.2) and the best value is 0.98 (18th image of sequence no. 1).

Fig. 6 shows the result of our developed method for the images corresponding to the highest and lowest M_{max} values. The tracked target window is represented in lighter intensity. We superimpose the proposed AVP model edges (coloured edges) inside the target window in each image. It is showed that the lowest values of M_{max} are obtained with the presence of contrast agent. However, template matching succeeded in finding the correct position. The other factor which affects the value of M_{max} is the orientation θ of the AVP. Fig. 6(d)-(f) shows the corresponding frames of each sequence to the lowest values of M_{max}. Despite of the the presence of contrast agent, the AVP model fits the edges of prosthesis. Such accurate results are obtained for all images of the three sequences.

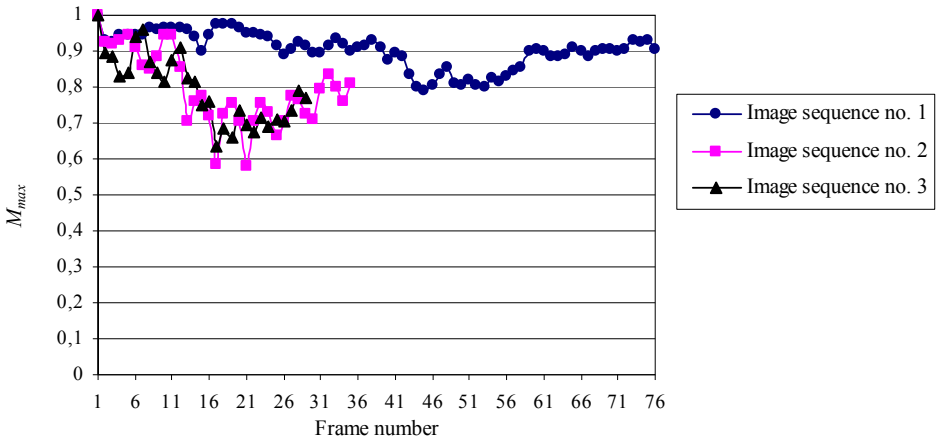

Fig. 5. Maximum normalized matching value (M_{max}) provided by the template matching algorithm and used for the localization of the AVP center for each frame of the three tested fluoroscopic image sequences.

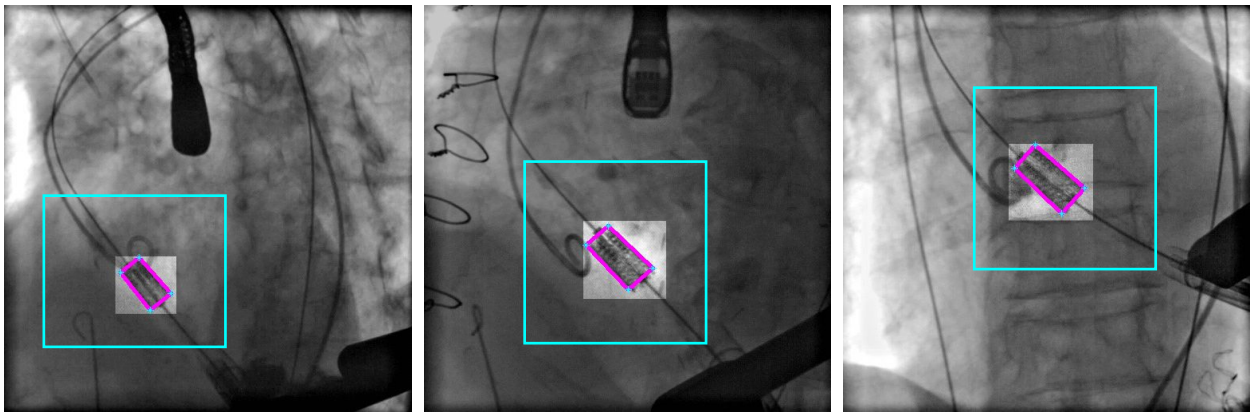

(a) 18th image of sequence no. 1 (b) 5th image of sequence no. 2 (c) 7th image of sequence no. 3

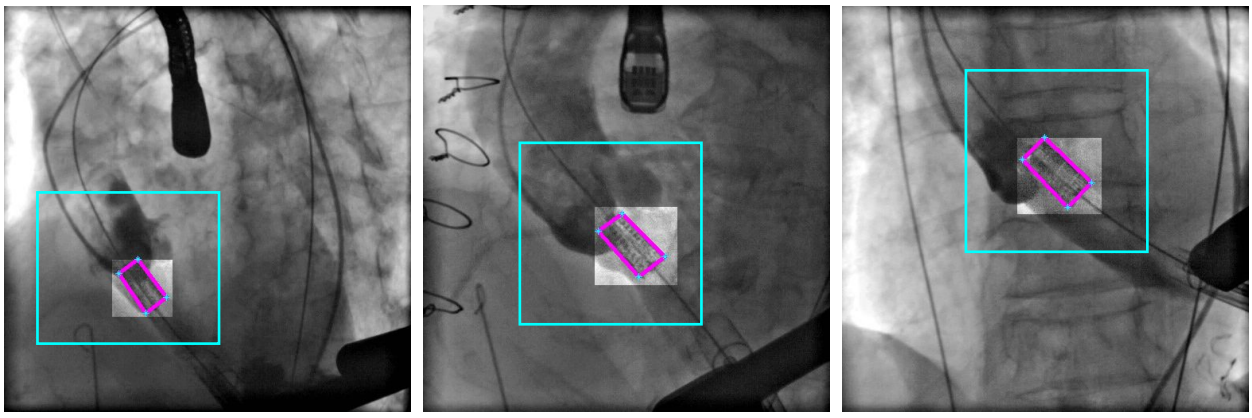

(d) 45th image of sequence no. 1 (e) 21st image of sequence no. 2 (f) 17th image of sequence no. 3

Fig. 6. Six different fluoroscopic images including the ROI and the AVP model which fits the prosthesis inside the target window (in lighter intensity) in two cases: (a)-(c) with the highest values of M_{max} which correspond to images without contract agent and (d)-(f) with the lowest values of M_{max} matching in the presence of contrast agent. The developed method is able to successfully localize the AVP in such difficult cases.

Moreover the error distance between the AVP position provided by our method and by a user determined was measured in each image sequence using Euclidian distance [11]. The error distance does not exceed 3 pixels (1.5 mm) in the three image sequences. Since the maximum allowed error is not yet established for this new surgical procedure, we assumed that it will be between 2 and 5 mm for TA-AVI. Our developed method is therefore clinically accepted.

Finally, the main advantage of our method is that it is not based on an accurate segmentation of the AVP. Searching two feature points of the AVP are easier than four corner points and faster. However a more complex shape of prosthesis will affect the estimatation of the model. By monitoring the position of AVP, it is possible to guide the surgeon to define easily the desired position of the AVP for this kind of implantation.

4. CONCLUSION

In this paper, we presented a new method for the AVP localization and tracking in 2D fluoroscopic image sequences during transapical minimally invasive aortic valve implantation. To do so, a template matching algorithm is used to track the AVP in the images. Based on a proposed AVP model, the prosthesis position is located in each image of sequence. The developed method is easy to use and requires user-interaction only at the beginning of algorithm. Accurate results are obtained despite of the background motion, the blurred vision, and the presence of contrast agent which may occlude the upper part of the prosthesis. Using this method, the AVP can be tracked correctly to assists the surgeon to improve the positioning of AVP for TA-AVI.
Further developments concern the possible use of different types of the AVP other than Edwards SAPIEN™ valve, the improvement of running time by optimizing the code and/or using hardware solutions and the clinical validation during the intervention. In addition, the coronary ostias will be localized to define automatically the safe zone of the implantation.

ACKNOWLEDGEMENT

This work is financially supported by the German Academic Exchange Service (DAAD) via scholarship number A0690520. Innovation Center Computer Assisted Surgery (ICCAS) at the University of Leipzig is funded by the German Federal Ministry for Education and Research (BMBF) and the Saxon Ministry of Science and Fine Arts (SMWK) in the scope of the initiative “Unternehmen Region” with grant numbers 03 ZIK 031 and 03 ZIK 032.

REFERENCES

[1] Walther, T., Dewy, T., Borger, M. A., Kempfert, J., Linke, A., Becht, R., Falk, V., Schuler, G., Mohr, F. W. and Mack, M., "Transapical aortic valve implantation: step by step," Ann. Thorac. Surg. 87(1), 276-383 (2009).

[2] Peters, T. M. and Cleary, K., [Image-Guided interventions: technology and applications], Springer, 1st ed., 50-53 (2008).

[3] Lin, C.-Y. and Ching, Y.-T., "Extraction of coronary arterial tree using cine x-ray angiograms," Biomed. Eng. Appl. Basis & Comm. 17(1), 111-120 (2005).

[4] Edwards Lifesciences, http://www.edwards.com/germany/products/percutaneousvalves/sapienthv.html, (2008).

[5] Schoonenberg, G., Schrijver, M., Duan, Q., Kemkers, R. and Laine, A., "Adaptive spatial-temporal filtering applied to x-ray fluoroscopy angiography," Proc. SPIE 5744, 870-878 (2005).

[6] Takemura, A., Hoffmann, K. R., Suzuki, M., Wang, Z., Rangwala, H. S., Harauchi, H., Rudin, S. and Umeda, T., "An algorithm for tracking microcatheters in fluoroscopy," Journal of Digital Imaging 21(1), 99-108 (2008).

[7] Palti-Wasserman, D., Bruckstein, A. M. and Beyar, R. P., "Identifying and Tracking a Guide Wire in the coronary arteries during angioplasty from X-ray images," IEEE Trans. on Biomed. Eng. 44(2), 152-164 (1997).

[8] Baert, S. A.M., Viergever, M. A. and Niessen, W. J., "Guide-Wire tracking during endovascular interventions," IEEE Trans. on Medical Imaging 22(8), 965-972 (2003).

[9] Goszczyńska, H., " Movement tracking of coronary artery segment in angiographic images sequences by template matching method-Computer recognition systems 2," Springer Berlin/Heidelberg, 45, 621-628 (2008).

[10] Vincent, L., "Morphological grayscale reconstruction in image analysis: applications and efficient Algorithms," IEEE Trans. on Image Processing 2(2), 176-201(1993).
[11] Gonzalez, R. C., Woods, R. E. and Eddins, S. L., [Digital image processing using MATLAB], Prentice Hall, 2nd ed. (2004).
[12] Lim, J. S., [Two-Dimensional signal and image processing], Englewood Cliffs, NJ, Prentice Hall, 548-550 (1990).
[13] Lewis, J. P., "Fast template matching," Vision Interface, 120-123 (1995).
[14] Ding, L., Goshtasby, A. and Satter, M., "Volume image registration by template matching," Image and Vision Computing 19(12), 821-832 (2001)
[15] Canny, J., "A computational approach to edge detection," IEEE Trans. on Pattern Analysis and Machine Intelligence 8(6), 679-698 (1986).